Accurate Determination of the Earth Tidal Parameters at the BIPM to Support the Watt Balance Project

O. Francis, Ch. Rothleitner, and Z. Jiang

Abstract

To achieve the targeted accuracy in the Bureau International des Poids et Mesures (BIPM) watt balance (WB) project, the value of g (acceleration due to gravity) must be known to an accuracy of 10^{-9} (10 nm/s^2) during the operation of balance. Gravity changes due to Earth Tides are the largest time variable signal affecting g at 10^{-7}. In order to improve the tidal prediction at the BIPM site, the relative spring gravimeter gPhone#032 collected observations for 6 months on site B of the BIPM. An analysis of the tidal results is presented here. We compare them with recent Earth and oceanic loading tidal models. In addition, using the gravity data from the Superconducting Gravimeter in Walferdange we demonstrate that a precision of +/−20 nm/s^2 can be achieved on the predicted value of g using a synthetic tide and including atmospheric pressure, polar motion and hydrological effects.

Keywords

Earth tides • Gravity • Spring gravimeter • Superconducting gravimeter • Watt balance

1 Introduction

Recently, several experiments and analyses of the spatial and temporal variations of the gravity field at the BIPM (see, Jiang et al. this issue) have been undertaken. The motivation for this work is to support the BIPM watt balance (WB) project. The WB project (Eichenberger et al. 2009) aims at determining Planck's constant, h, for the future realization of a new definition of the kilogram. This new definition is based on the Planck's constant and on the accurate knowledge of the acceleration due to gravity. The requirement on the accuracy of the instantaneous value of g for this project is 10^{-8}. This could be achieved either by simultaneously operating the watt balance and an absolute gravimeter or by accurately predicting the g-value. In the latter case, this would mean that all modeled contributions to the g-value should be determined at 10^{-9} or with an accuracy of 10 nm/s^2 (i.e. one order of magnitude less than the desired precision).

The largest time varying gravity signals at any location are the Earth tides. Gravity perturbations due to these tides can have peak-to-peak amplitudes of up to 2,500 nm/s^2. [For an excellent and comprehensive review on the subject of Earth tides, the reader is referred to Agnew (2007).] The Earth tides include two contributions: the body tides which are the tidal deformations on the ocean-less solid Earth; and, the loading and attraction effects of the ocean tides. The tidal gravity effect consists of three terms: the direct vertical component of the tidal force due to the Moon and the Sun, the changes in gravity due to the vertical displacement of the station and due to the potential change caused by the redistribution of the mass of the deformed Earth. Moreover, as both the body tide and ocean tide contributions are caused by the luni-solar attraction, they both contain the same frequencies. From the spectral analysis of the observations, it is not possible to distinguish the contribution of the individual components.

O. Francis (✉) • Ch. Rothleitner
Faculty of Science, Technology and Communication, University of Luxembourg (UL), Luxembourg City, Luxembourg
e-mail: olivier.francis@uni.lu

Z. Jiang
Bureau International des Poids et Mesures (BIPM), Pavillon de Breteuil, 92312 Sèvres Cedex, France

C. Rizos and P. Willis (eds.), *Earth on the Edge: Science for a Sustainable Planet*, International Association of Geodesy Symposia 139, DOI 10.1007/978-3-642-37222-3_42,

The gravity effect of the body tides can be computed to an accuracy of about 3 nm/s^2 on the basis of an Earth model determined from seismology. On the other hand, the direct attraction and loading effect of the ocean tides are less precise due to inaccuracies in the ocean tide models. It is thus difficult to assess the uncertainty of the tidal prediction itself. The best practice is to model the full tidal signal. This method consists of observing the gravity tides with a well calibrated gravity meter. From these observations, the tidal waves amplitude and phases (their number depending on the length of the recordings) are estimated in a least-square's adjustment. The amplitudes and phases can be then used to predict the tides in combination with the tidal generating potential, so-called synthetic tides.

In a recent study, Ducarme (2009) demonstrated that in the best case the accuracy of tidal predictions that are based on observations of 5×10^{-4} (i.e. 1.25 nm/s^2) is "the limit of accuracy using long time series of observations of regularly calibrated instruments". The contribution of the present paper is to provide the best tidal prediction at the BIPM site using 6-months of continuous data from a well calibrated relative spring gravimeter. The precision of the observed tidal parameters is evaluated by comparing the observations with Earth tides and ocean tidal loading models.

To illustrate how precisely gravity can be predicted, we investigate the tide-free observations from the Walferdange superconducting gravimeter OSG-040. The residual gravity signal after subtracting the tides can be explained in terms of atmospheric pressure effects, the variation of the centrifugal acceleration due to the polar motion and attraction and loading effects caused by variations in the regional water storage. We find that the residuals (after removing a tidal prediction) of the observed gravity is less than 20 nm/s^2. Although this value is twice our original target, it is sufficient for the Watt Balance Experiment.

2 Observations

Before installing the spring gravimeter gPhone#032 at the BIPM, the instrument was operated in Walferdange (Luxembourg) side-by-side with the superconducting gravimeter (SG) OSG-040. The SG has been calibrated with respect to the absolute gravimeter FG5#216 with a precision of 0.1 %. The calibration factor of the gPhone was estimated by comparing with the SG data of the same precision. After the BIPM observations, the gPhone calibration was again checked against the SG in Walferdange. The comparison showed that the calibration factor of the gPhone did not change.

The gPhone#032 observed gravity continuously on the B pillar at the BIPM from 01-04-2010 to 11-10-2010. The instrument was installed on a tripod (Fig. 1) built in our laboratory. The tripod is able to maintain the verticality of the gravimeter. Unfortunately, the tilt control system failed at the end of August 2011 for some unknown reason. As a result, 4 days of observations were lost. This has a minor effect on the tidal results as the software we used, ETERNA (Wenzel 1996) is designed to process discontinued time series. The top panel of Fig. 2 shows the 187-day record of the raw gravity data; the bottom panel shows the local atmospheric pressure observations. The gravity record shows a small quasi-linear instrumental drift of about 4 nm/s^2/day. This drift will not affect the tidal analysis as the raw data are high-pass filtered before adjusting the observations for the tidal harmonic components.

Fig. 1 The spring gravimeter gPhone#032 on its tilt controlled tripod and electronics

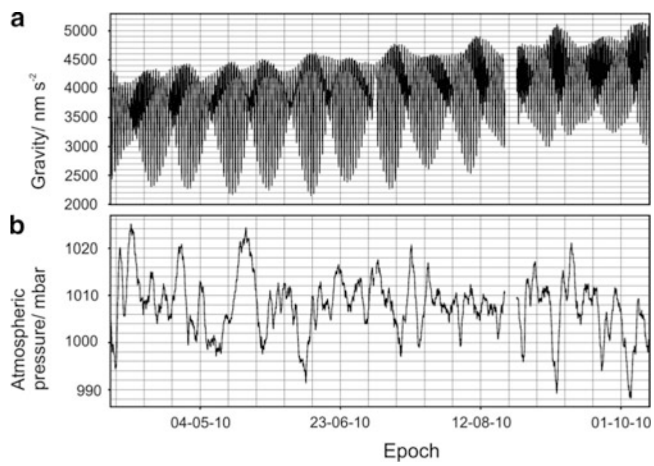

Fig. 2 (**a**) Raw gravity data of the gPhone#032 spring gravimeter; (**b**) atmospheric pressure observations. Both records from the BIPM (Paris, France) from 01-04-2010 to 11-10-2010

3 Tidal Analysis

The raw 1-s data (Fig. 2a) were edited for spikes and other non-tidal disturbances primarily due to earthquakes using Tsoft (van Camp and Vauterin 2005). The corrected data

Table 1 Tidal parameters at BIPM (Sèvres, France) estimated using 187-days of observations taken with the gPhone#032 (from 01/04/2010 to 11/10/2010)

Wave	Start frequency (cpd)	End frequency (cpd)	Amplitude (nm/s^2)	Amplitude factor	Standard deviation	Phase lead (degree)	Standard deviation (degree)
Q_1	0.721500	0.906315	67.514	1.1453	0.0007	−0.48	0.04
O_1	0.921941	0.940487	351.958	1.1431	0.0001	0.04	0.01
M_1	0.958085	0.974188	27.690	1.1435	0.0014	0.25	0.08
P_1	0.989049	0.998028	164.033	1.1450	0.0003	0.32	0.02
K_1	0.999853	1.011099	490.796	1.1334	0.0001	0.43	0.01
J_1	1.013689	1.044800	27.908	1.1525	0.0018	0.28	0.10
OO_1	1.064841	1.216397	15.300	1.1549	0.0026	−0.01	0.15
$2N_2$	1.719381	1.872142	11.200	1.1249	0.0032	4.02	0.18
N_2	1.888387	1.906462	72.017	1.1551	0.0006	4.00	0.04
M_2	1.923766	1.942754	385.481	1.1838	0.0001	3.24	0.01
L_2	1.958233	1.976926	10.348	1.1242	0.0060	2.98	0.34
S_2	1.991787	2.002885	180.745	1.1930	0.0003	1.25	0.02
K_2	2.003032	2.182843	49.231	1.1955	0.0009	1.55	0.05

were then decimated to hourly data by applying a low-pass filter with a cutoff period of 2 h. An Earth tidal analysis was performed using the ETERNA software in which the tidal parameters, the amplitude factor (delta factor) and phase (alpha), are estimated simultaneously with the barometric admittance factor.

The results of the tidal analysis are presented in Table 1. Due to the limited length of the time series, it was possible to recover only 13 tidal waves in the diurnal and semidiurnal bands. For the other tidal bands, including the long-period band, one must rely on modeled tidal parameters. In Sèvres, the long-period gravity tidal signal varies between −100 and +50 nm/s^2. Assuming an uncertainty of 1 % (Ducarme et al. 2004), the uncertainty on the tidal prediction is less than 1 nm/s^2.

The tidal analysis also provides an estimate of the error on the amplitude and phase determined for the different waves. For the waves with the larger amplitude, the one-sigma uncertainty on the amplitude factor is less than 0.02 %. Figure 3 shows the synthetic tides (top panel) and their associated 2-sigma uncertainty (bottom panel) for 1 month at Sèvres. The uncertainty is time dependent and varies between −0.6 and 0.5 nm/s^2 for a tidal signal that ranges between +/−1,000 nm/s^2. As the precision of the calibration factor is 0.1 %, the associated error can reach up to 2 nm/s^2. This result means that the precision of the tidal prediction is completely dependent on the precision of the gravimeter calibration.

In Table 2, the observed tidal parameters are compared with the sum of an elastic oceanless body tide Earth model and a calculated oceanic attraction and loading effect. The final residuals for the main waves are around a few nm/s^2, which is the best one could achieve (see Ducarme 2009, for example).

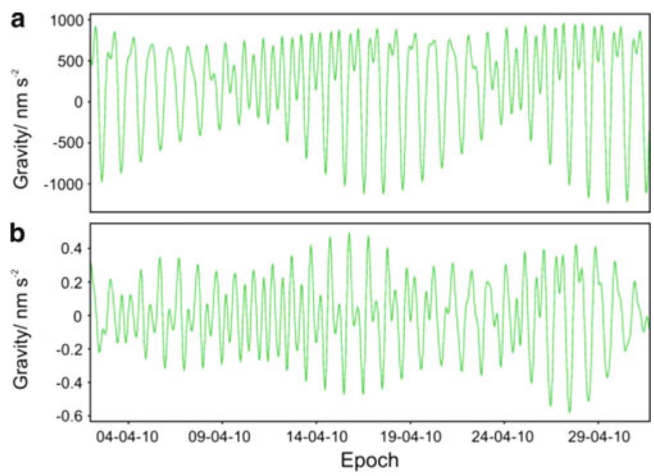

Fig. 3 (**a**) One month of predicted gravity tides for the BIPM in Sèvres; (**b**) the associated 2-sigma uncertainty determined using the observed tidal parameters. Note the scale difference between the *top* and *bottom panels*

In Fig. 4, the observed tidal factors are compared with the state-of-the art theoretical tides model of Dehant et al. (1999). Two different oceanic tides models were used to calculate the oceanic loading effect. From Fig. 4, we conclude that the CSR3.0 (Eanes and Bettadpur 1995) model provides an almost perfect match with the observations. The FES2004 (Lyard et al. 2006) model provides systematically low delta factors. The results in Fig. 4 demonstrate the difficulty of selecting the correct ocean tides model particularly if no gravity observations are available to validate the choice.

One might argue that the calibration factor used for the gravity meter is too high. By lowering the calibration, the FES2004 model would fit the observations better than the CSR3.0. The only response, as stressed in Ducarme (2009),

Table 2 **A**(A,α) is the observed tidal response; **R** (R,0) elastic oceanless Earth model response (calculated); **B**(B, β) = **A**-**R; L**(L,λ) oceanic attraction and loading vector (calculated with the CSR3.0 ocean tides model); **X**(X,χ) = **B**–**L** = **A**–**R**–**L** is the final residue vector

Wave	A (nm/s²)	α (degree)	R (nm/s²)	B (nm/s²)	β (degree)	L (nm/s²)	λ (degree)	X (nm/s²)	χ (degree)
Q_1	67.51	−0.48	68.1	0.8	−133.6	0.8	246.2	0.3	141.5
O_1	351.96	0.04	355.4	3.5	175.5	2.3	167.8	1.3	−170.6
P_1	164.03	0.32	164.7	1.1	123.2	1.4	83.3	0.9	−146.0
K_1	490.80	0.43	491.3	3.7	98.0	4.2	75.8	1.6	−165.2
N_2	72.02	4.00	72.39	5.1	96.9	4.9	91.0	0.5	166.4
M_2	385.48	3.24	378.3	22.7	73.4	21.8	73.5	0.9	71.9
S_2	180.75	1.25	176.1	6.1	40.2	7.3	45.0	1.3	−112.4
K_2	49.23	1.55	47.9	1.9	44.4	1.9	43.5	0.0	139.3

The other waves are not considered here as ocean tides models are not available for those. A graphical representation of these parameters can be found in Melchior (1983)

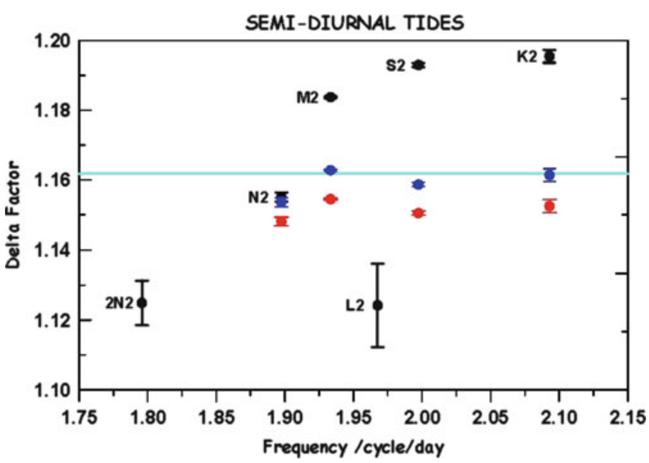

Fig. 4 Observed tidal parameters (*black dots*) at the BIPM estimated from the analysis of 187-day record of the gPhone#032. The *red* and *blue dots* are the observed delta factors corrected for ocean loading and attraction using the FES2004 and CSR3.0 oceanic tides models, respectively. The *blue line* represents the Dehant et al. (1999) Earth tide model

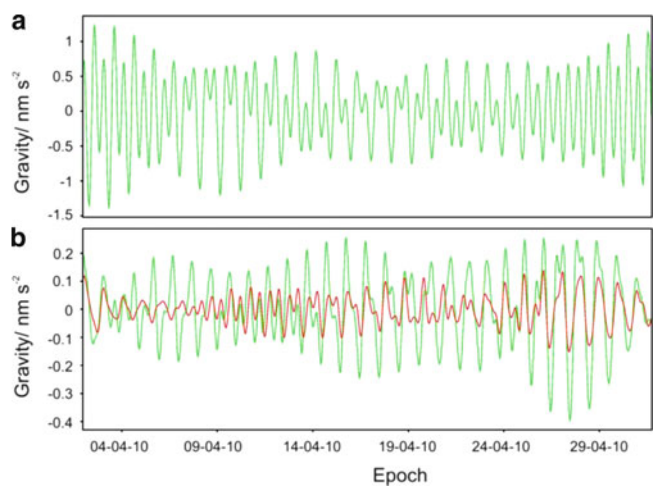

Fig. 5 (**a**) The difference between Earth tides predicted using the observed tidal parameters estimated using 6 months of data and 4 years of data from the superconducting gravimeter in Walferdange (Luxembourg); (**b**) the uncertainties (2-sigma) of both predictions (6-month in *green*, 4-year in *red*) using the a posteriori errors (columns 6 and 8 from Table 1) of the tidal analysis

is to have an independently and well-calibrated gravimeter as was the case for this experiment (see Sect. 2).

4 Discussion

In this section, we investigate the potential benefit on the estimate of the tidal parameters due to increasing the duration of the gravity observations. For this analysis, we use 4-years of data from the superconducting gravimeter in Walferdange. We compare the synthetic tides generated with the tidal parameters estimated from 6-month with those estimated from 4-year of observations, respectively. The differences, Fig. 5, are around +/−1 nm/s². However, it is interesting to note that the uncertainties calculated from the a posteriori errors (i.e. columns 6 and 8 from Table 1) of the tidal analysis are too optimistic.

The same SG data from Walferdange (Fig. 6) are used to determine how precisely the g value can be predicted. First, the raw observations are corrected for a synthetic tide, the atmospheric pressure effect (using an admittance factor of 3 nm/s² per mbar), and polar motion using the pole position published by the IERS (REF). The order of magnitude of each of these corrections is: +1,000 to −1,500 nm/s², +60 to −100 nm/s² and +40 to −40 nm/s², respectively. The gravity residuals after applying the above corrections vary between +40 and −60 nm/s². The variability of the regional water storage is the main contributor to these residual gravity signals. Lampitelli and Francis (2009) developed a simple model based on rain gauge observations to estimate gravity variations due to this component. The water storage effect varies from −10 to −80 nm/s². The final residuals—corresponding to the precision obtained on the prediction of g—vary between −20 and +20 nm/s².

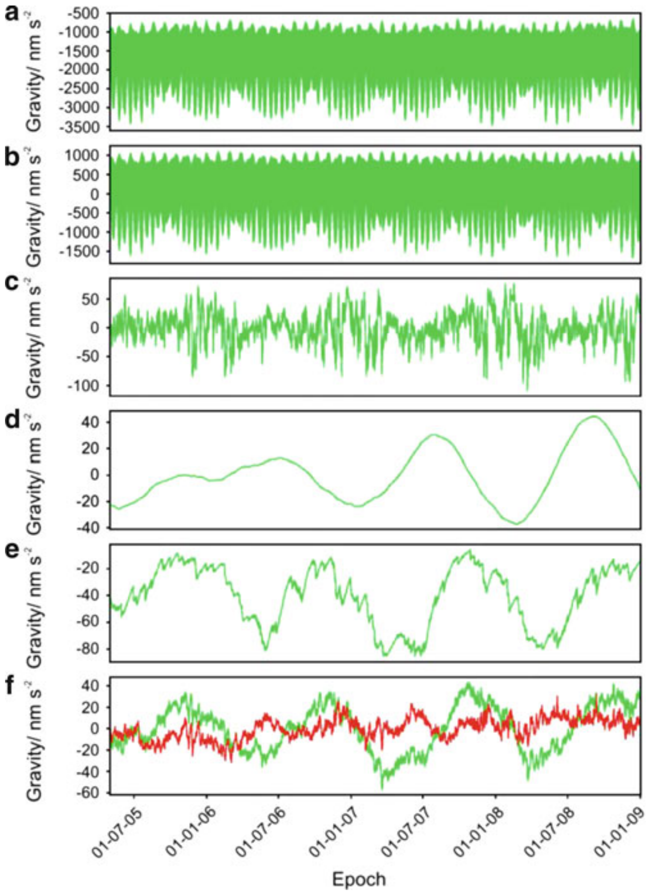

Fig. 6 (**a**) Raw gravity observations from the superconducting gravimeter in Walferdange (Luxembourg); (**b**) synthetic tides using observed tidal parameters; (**c**) atmospheric pressure effect; (**d**) polar motion effect; (**e**) regional water storage effect estimated using rain gauge data (Lampitelli and Francis 2009); (**f**) the residuals with (*red*) and without (*green*) the water storage correction

The residuals could be further reduced up to some 10 nm/s^2 by calculating the atmospheric effect using a three-dimensional atmospheric pressure model (Neumeyer et al. 2004). However, this requires far more computation time.

5 Conclusions

Tidal parameters obtained with the gPhone#032 are a factor 10 more precise than previous determinations of tidal parameters obtained with the LaCoste-Romberg 906 spring gravimeter (Robertsson et al. 2001). In addition, our results are closer to Earth tide models and the attraction and loading of the ocean tides. This result is due to a more stable and accurate temperature control of the gravity sensor, improvements in the instrument electronics, a careful calibration of the gravimeter and the tilt compensation of the gravimeter using our in-house tripod. We show that 6 months of continuous gravity observations provide us with tidal parameters that are sufficiently accurate to allow us to predict the tides with a precision of a few nm/s^2. The dominant source of uncertainty is the error on the calibration factor that is determined in the best case with a relative precision of 10^{-3}.

Using SG observations from the gravity station in Walferdange, we demonstrate that it is possible to predict the g-value with a precision of +/−20 nm/s^2 from: (1) reliable observed tidal parameters; (2) continuous measurements of the atmospheric pressure at the site; (3) the pole position as published by the IERS (Petit and Luzum 2010); and, (4) a comprehensive regional water storage model (as for example those presented in Lampitelli and Francis 2009 or Van Camp et al. 2006).

Overall, our gravity tide prediction that is based on observed tidal parameters attains a precision of 10 nm/s^2. The limiting factor in the precision of the prediction is the precision of calibration factor of the spring gravimeter. However, the models for predicting other geophysical signals (like water storage effects) still do not reach that level.

References

Agnew DC (2007) Earth tides. In: Herring TA, Schubert G (eds) Treatise on geophysics: geodesy. Elsevier, New York, pp 163–195

Dehant V, Defraigne P, Wahr JM (1999) Tides for a convective Earth. J Geophys Res 104(B1):1035–1058

Ducarme B (2009) Limitations of high precision tidal prediction. Bull d'Inform Marées Terrestres 145:11663–11677

Ducarme B, Venedikov AP, Arnoso J, Viera R (2004) Determination of the long period tidal waves in the GGP superconducting gravity data. J Geodyn 38:307–324

Eanes RJ, Bettadpur S (1995) The CSR 3.0 global ocean tide model. Technical Memorandum CSR-TM-95-06. Center for Space Research, University of Texas, Austin

Eichenberger AG, Genevès G, Gournay P (2009) Determination of the Planck constant by means of a watt balance. Eur Phys J Spec Top 172:363–83

Lampitelli C, Francis O (2009) Hydrological effects on gravity and correlations between gravitational variations and level of the Alzette River at the station of Walferdange, Luxembourg. J Geodyn. doi:10.1016/j.jog.2009.08.003

Lyard F, Lefevre F, Letellier T, Francis O (2006) Modelling the global ocean tides: modern insights from FES2004. Ocean Dyn 56:394–415. doi:10.1007/s10236-006-0086-x

Melchior P (1983) The tides of the planet earth. Pergamon, Oxford

Neumeyer J, Hagedoorn J, Leitloff J, Schmidt T (2004) Gravity reduction with three-dimensional atmospheric pressure data for precise ground gravity measurements. J Geodyn 38:437–450

Petit G, Luzum B (2010) (eds) IERS Technical Note 36. Verlag des Bundesamts für Kartographie und Geodäsie, Frankfurt am Main, 179 pp. ISBN 3-89888-989-6

Robertsson L, Francis O, van Dam T, Faller J, Ruess D, Delinte J-M, Vitushkin L, Liard J, Gagnon C, Guo You Guang, Huang Da Lun, Fang Yong Yuan, Xu Jin Yi, Jeffries G, Hopewell H, Edge R, Robinson I, Kibble B, Makinen J, Hinderer J,Amalvict M, Luck B, Wilmes H, Rehren F, Schmidt K, Schnull M, Cerutti G, Germak A, Zabek Z, Pachuta A, Arnautov G, Kalish E, Stus Y, Stizza D, Frederich J, Chartier J.-M, Marson I (2001) Results from the fifth international comparison of absolute gravimeters, ICAG97. Metrologia 38:71–78

Van Camp M, Vauterin P (2005) Tsoft: graphical and interactive software for the analysis of time series and Earth tides. Comput Geosci 31(5):631–640

Van Camp M, Vanclooster M, Crommen O, Petermans T, Verbeeck K, Meurers B, van Dam T, Dassargues A (2006) Hydrogeological investigations at the Membach station, Belgium, and application to correct long periodic gravity variations. J Geophys Res 111:B10403. doi:10.1029/2006JB004405

Wenzel H-G (1996) The nanogal software: Earth tide data processing package: ETERNA 3.3. Bull d'Inform Marées Terrestres 124:9425–9439